

## Anisotropy-induced optical transitions in PbSe and PbS spherical quantum dots

A. D. Andreev\*

*A. F. Ioffe Physico-Technical Institute, Polytechnicheskaja 26, St. Petersburg, 194021, Russia*

A. A. Lipovskii†

*St. Petersburg State Technical University, Polytechnicheskaja 29, St. Petersburg, 195251, Russia*

(Received 5 October 1998)

Optical-absorption spectra of PbSe and PbS spherical quantum dots have been studied both theoretically and experimentally. Exact theoretical analysis of the energy spectra and optical transitions has been carried out in the framework of four-band  $\mathbf{k}\cdot\mathbf{p}$ -method with full account of the anisotropy effects. It is demonstrated that strong anisotropy of the energy bands of bulk PbSe and PbS results in pronounced optical transitions in quantum dots, which are forbidden in isotropic approximation. These anisotropy-induced transitions have been clearly observed in the measured absorption spectra of the PbSe and PbS quantum dots.

[S0163-1829(99)11415-2]

Glasses embedded with semiconductor quantum dots (SQD) are of interest for the studies of basic properties of the low-dimensional structures and their quantum confined optical transitions. Dependence of the transition energy on the SQD size allows the “tuning” of the glasses to wavelength of a specific light source if the energy of photons at a desirable wavelength exceeds the energy gap of the bulk semiconductor, and resonance “tuning” is possible if the SQD are narrowly size distributed. The studies of the SQD in glasses were mainly performed with wideband II-VI semiconductors with the energy gap corresponding to the visible range of optical wavelengths.<sup>1</sup> The synthesis of the glasses embedded with semiconductor quantum dots and modeling of these SQD have recently been performed.<sup>1-9</sup> In particular, the theory allowing description of optical properties of II-VI and III-V SQD was developed by Efros and co-workers.<sup>7-9</sup> The energy spectra and optical transition matrix elements in IV-VI SQD (PbSe and PbS) have been calculated in isotropic approximation taking account of anisotropic effects only in the framework of first-order perturbation theory. However, as is shown in the present paper, the anisotropy of the energy bands strongly affects the optical properties of PbSe and PbS SQD and, therefore, should be taken into account in full degree.

In this paper we present our results of theoretical and experimental study of the electronic structure and optical transitions in spherical PbSe and PbS SQD. It is shown, that full account of the anisotropy effects provides good description of the experimental optical-absorption spectra and identification of the observed transitions including transitions, which nature is not clear within isotropic approximation or previous theory developed by Kang and Wise.<sup>3</sup>

We used the recently designed  $\text{P}_2\text{O}_5\text{-Na}_2\text{O-ZnO-AlF}_3\text{-Ga}_2\text{O}_3$  glass system<sup>4,5</sup> doped with PbS or PbSe for formation of the semiconductor quantum dots via phase decomposition of oversaturated solid solutions of the IV-VI semiconductors in the glass matrix. The glasses were synthesized at  $\sim 1100^\circ\text{C}$ , the glass transition temperature  $T_G \sim 380^\circ\text{C}$ . The technique of raw batch was applied. After the synthesis and the quenching at room temperature, the glass samples were slightly yellowish that is typical for

lead-containing glasses. Thermal treatment of the glasses at  $390\text{--}400^\circ\text{C}$  led to their coloring to brown and black depending on the duration and the temperature of the annealing. X-ray diffractometry and transmission electron microscopy of the annealed glass samples demonstrated the existence of spherical PbS and PbSe quantum dots within the glass matrix. Size of the quantum dots varied between  $\sim 2$  and  $15\text{ nm}$  depending on the duration and the temperature of the annealing of the samples. Evaluated width of the narrowest size distribution of the quantum dots is  $\sim 5\text{--}7\%$ . This narrow size distribution of SQD formed in glasses is a unique one, except SQD formed by Borrelli and Smith<sup>2</sup> in a silicate glass, and it is closer to the distributions typical for SQD formed with chemical techniques.<sup>6</sup>

The optical-absorption spectra of the annealed glass samples with PbS and PbSe quantum dots were measured in the spectral range  $350\text{--}3500\text{ nm}$  at room and at liquid-helium temperatures. Due to the narrow size distribution of the SQD, sets of optical-absorption peaks corresponded to different quantum transitions were clearly observed even in the spectra measured at room temperature. The measurements performed at He temperature indicated narrow absorption peaks corresponding to the narrow size distribution. Increase of the annealing duration leads to the motion of the SQD-doped glass spectra from the spectrum of the unannealed glass towards the spectrum of the bulk IV-VI semiconductor crystals.

To calculate the energy levels and the wave functions of electrons and holes in spherical SQD, we used four-band  $\mathbf{k}\cdot\mathbf{p}$  model, which takes account of anisotropy and accurately describes the band structure near the  $L$  point of the Brillouin zone.<sup>10,11</sup> Contrary to calculations performed by Efros and co-authors<sup>7-9</sup> for III-V and II-VI SQD, which have band edge at  $\Gamma$  point of the Brillouin zone, we use the  $L$ -point expansion in the  $\mathbf{k}\cdot\mathbf{p}$  model since the conduction-band minimum and valence-band maximum in PbS and PbSe are located in the  $L$  point of the  $k$  space. This four-band  $\mathbf{k}\cdot\mathbf{p}$  model takes into account coupling of the conduction and valence bands, which was shown to be important for the energy-level calculations in isotropic approximation.<sup>3</sup> We represent the Hamiltonian  $\hat{H}$  of the  $\mathbf{k}\cdot\mathbf{p}$  model as  $H = H_{\text{isotr}}$

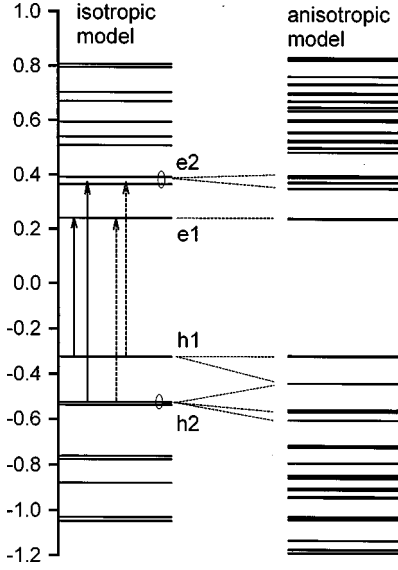


FIG. 1. Energy levels of PbSe SQD calculated in isotropic approximation (left-side horizontal lines) and with full account of anisotropy (right-side lines). Vertical solid and dashed lines on left-side diagram indicate permitted and forbidden transitions in isotropic approximation, respectively. Dotted lines from left-side levels to the right-side ones show isotropic states which give the main contribution to the formation of the real SQD levels, SQD radius  $a=40$  Å, and temperature  $T=12$  K.

+  $H_{\text{an}}$ , where the first term is the isotropic part and the second term describes the anisotropy effects.<sup>3</sup> The carrier wave functions in spherical SQD, i.e., the eigenfunctions of  $\hat{H}$ , are expanded in the series of the eigenfunctions  $|\alpha\rangle$  of Hamiltonian  $H_{\text{isotr}}$  corresponding to the isotropic SQD problem:

$$\Psi = \sum_{\alpha} C_{\alpha} |\alpha\rangle, \quad (1)$$

where the sum is taken over all states  $\alpha$  of the isotropic Hamiltonian (with account of degeneracy). Then the coefficients  $C_{\alpha}$  in Eq. (1) and the energy levels of SQD are calculated numerically as the solution of the eigenvalue problem for the matrix  $H_{\alpha\beta} = \delta_{\alpha\beta} E_{\alpha} + \langle \alpha | \hat{H}_{\text{an}} | \beta \rangle$ , where  $\hat{H}_{\text{isotr}} |\alpha\rangle = E_{\alpha} |\alpha\rangle$ , and  $E_{\alpha}$  is the energy of the states  $\alpha$ . The matrix elements  $H_{\alpha\beta}$  are calculated analytically using Wigner-Eckart theorem<sup>12</sup> and explicit expression for functions  $|\alpha\rangle$  through spherical harmonics and Bessel functions.<sup>3,13</sup> Matrix elements for optical transitions between two levels  $i$  and  $f$  in SQD are calculated using the formula

$$M_{i \rightarrow f} = \sum_{\alpha, \beta} [C_{\alpha}^{(i)}]^* C_{\beta}^{(f)} M_{\alpha\beta}, \quad (2)$$

where optical matrix element between isotropic states  $\alpha$  and  $\beta$ ,  $M_{\alpha\beta}$ , is calculated analytically. Finally, the square of the matrix element for a given polarization obtained using Eq. (2) is averaged over the directions of the polarization vector assuming uniform distribution for the orientation of the spherical SQD in glass matrix. Also, we note that if we restrict the summation in Eq. (1) only over the degenerate (or quasidegenerate) states with a given energy, then we will simply get the result of first-order perturbation theory obtained in Ref. 3. However, this approximation is not valid because of strong mixing of isotropic states with different

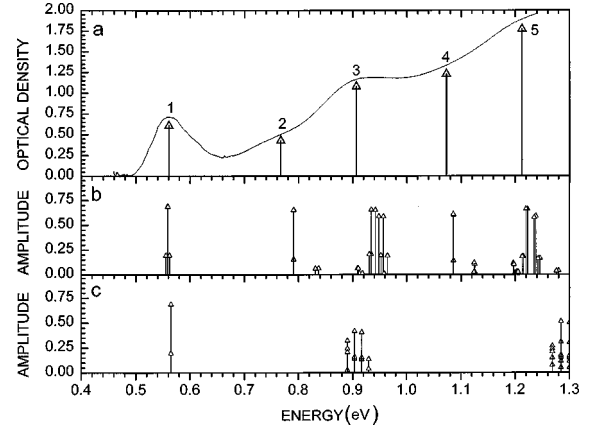


FIG. 2. Measured optical-absorption spectra of the glass sample embedded with PbSe quantum dots; arrows show the transition energy positions obtained from the analysis of the second derivative (a), the square of the transition matrix element averaged over polarizations (transition amplitude) calculated using full account of the band anisotropy (b), and in isotropic model (c). The SQD radius  $a=40$  Å; for calculations we used the following parameters:  $E_g(T=12 \text{ K})=0.166$  eV,  $2P_i^2/m=1.7$  eV,  $2P_i^2/m=3.0$  eV,  $m/m_i^- = 4.3$ ,  $m/m_i^- = 3.1$ ,  $m/m_i^+ = 8.7$ , and  $m/m_i^+ = 3.3$  (notations of parameters are the same as in Ref. 3).

energies, which results in nonzero optical matrix elements for some additional transitions, which are not permitted within the framework of the isotropic model.

Figure 1 shows the energy levels of spherical SQD calculated using isotropic and anisotropic models. The energy of the ground states in the isotropic and anisotropic models are close, but not identical. The anisotropy does not change significantly the energy position of the ground state since we have used an average set of band parameters for the isotropic model:<sup>3</sup>  $P^2 = (2P_i^2 + P_j^2)/3$ ,  $3/m^{\pm} = 2/m_i^{\pm} + 1/m_j^{\pm}$  (notations are the same as in Ref. 3). In isotropic approximation each quantum state in SQD can be labeled by four quantum numbers:<sup>3</sup>  $|\alpha\rangle = |j, m, \pi, n_r\rangle$ , where  $j$  and  $m$  are the angular momentum numbers,  $n_r$  is the radial quantum number, and  $\pi$  denotes the parity. Ground electron and hole levels (**e1**, **h1**, see Fig. 1) consist of the states with  $j=1/2$ ,  $\pi=\theta$ , and  $n_r=1$ , and higher level **e2**, **h2** groups consist of the states with  $j=1/2, 3/2$ ,  $\pi=-\theta$ , and  $n_r=1$  (here  $\theta=1$  for electrons, and  $\theta=-1$  for holes). For isotropic case the selection rules for the direct optical transitions are the following:  $\Delta j=0, \pm 1$ ;  $\Delta m=0, \pm 1$ ; and  $\pi_e \pi_h = -1$ . Therefore all optical transitions between level groups **e1** ↔ **h2** and **e2** ↔ **h1** (dashed lines on Fig. 1) are forbidden in isotropic model because of a parity reason. The analogous conclusion is also valid for the transitions between higher levels. However, the situation considerably changes in the case when the anisotropy of the energy bands is taken into account. The influence of the anisotropy results in two main effects. First, the energy levels are split and shifted (see Fig. 1). Second, the strong mixing of different isotropic states takes place. Therefore, the transitions, which are forbidden in isotropic approximation, become allowed to a degree of this mutual mixing. These transitions are clearly observed in measured spectra (see Figs. 2 and 3). Thus the anisotropy of the energy bands substantially affects the optical-absorption spectra of SQD.

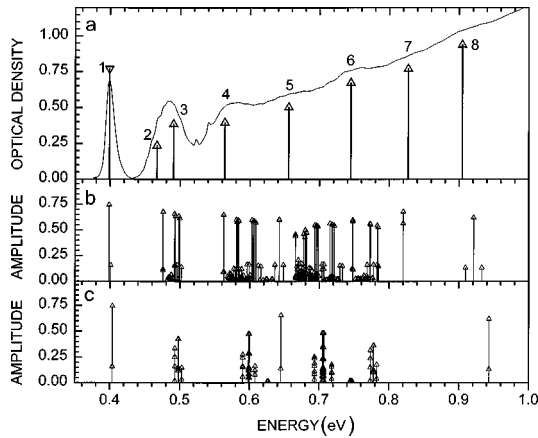


FIG. 3. The same as Fig. 2, but for PbS SQD of radius  $a = 73 \text{ \AA}$ . For calculations we used the following parameters:  $E_g(T=12 \text{ K}) = 0.299 \text{ eV}$ ,  $2P_t^2/m = 1.4 \text{ eV}$ ,  $2P_l^2/m = 3.3 \text{ eV}$ ,  $m/m_t^- = 1.3$ ,  $m/m_l^- = 2.9$ ,  $m/m_t^+ = 1.6$ , and  $m/m_l^+ = 2.9$ .

Figure 2(a) shows measured absorption spectrum of PbSe SQD at  $T=12 \text{ K}$ . The second derivative analysis of this spectrum allows us to distinguish five absorption bands corresponding to optical transitions or groups of transitions. The isotropic model and the model of Ref. 3 can predict the energy position of only three transitions [see Fig. 2(c)], because the other ones are forbidden in these simple models. The calculations in the framework of an accurate anisotropic model show that the amplitudes of the additional transitions (labeled as 2 and 4 in Fig. 2) are of the same order as the amplitudes of the transitions allowed in an isotropic model. The energies for the transitions 1–5 calculated in anisotropic model are in good agreement with experiment (see Fig. 2). The discrepancy of theoretical results and experimental data is less than 20–30 meV, which is possibly due to the influence of such factors as the deviation from spherical shape of the SQD, effects of interface, and some uncertainties in material parameters. To estimate the effect of deviation from the spherical shape on the absorption spectra of SQD's, we performed calculations of the energy shifts induced by the geometry of QD's in case they were ellipsoidal with semiaxes  $a_1$  and  $a_2$ . Using the methods of perturbation theory similar to that described in Refs. 8 and 14, we obtained that the energy shift caused by such changing of the SQD shape is given by  $\Delta E_\alpha = \delta_a E_\alpha C_\alpha$ , where  $\delta_a = 2(a_1 - a_2)/(a_1 + a_2)$  is

the degree of deviation from the spherical shape,  $E_\alpha$  is the energy of state  $\alpha$  in spherical SQD, and  $C_\alpha$  is the coefficient that depends on the quantum numbers  $\alpha = (j, m, \pi, n_r)$ . Estimating from the TEM measurements<sup>5</sup> the value of  $\delta_a$  to be less or equal to 0.05,  $\delta_a \leq 0.05$ , we found that the energy shift is less than 5 meV and 12 meV for the PbS and PbSe SQD, respectively. Therefore the effect of deviation of the SQD shape from sphere is much smaller than the effect of anisotropy, and it is also not the cause of appearance of the observed transition in the absorption spectra.

Measured absorption spectrum of PbS SQD is plotted in Fig. 3(a). For PbS the first additional transition 2 is closer to the second one 3 permitted in the isotropic model (see Fig. 3) than in the case of PbSe SQD's (Fig. 2), which is due to weaker anisotropy of the energy bands in PbS compared to PbSe. Rather wide peak 4 and plato consist of several transitions, which correspond to the slightly shifted transitions between energy levels calculated for the isotropic model, and one additional transition (low-energy side). Note that the isotropic model predicts the energy position of peak 4 to be 40 meV larger than the experimental one. The higher energy peculiarities of 5–8 in absorption spectrum cannot be identified synonymously because for these transitions the effect of the factors mentioned above is rather strong. However, we can conclude that weak peak 7 most likely is due to additional transitions, while peak 8 is induced by the transition permitted in the isotropic model, and peaks 5 and 6 consist of both types of transitions. Thus, we manage to observe and interpret up to eight transitions in PbS SQD.

In conclusion we note that we have developed a theoretical model with full account of anisotropy of the energy bands. The model describes properly the measured absorption spectra of PbSe and PbS spherical SQD. This model allows us to identify up to five transitions in PbSe and up to eight transitions in PbS SQD. It is demonstrated that optical transitions, which are forbidden in isotropic model, become allowed when the anisotropy is included in the model in full degree. These anisotropy-induced additional optical transitions have been clearly observed in the measured absorption spectra of narrowly distributed PbSe and PbS SQD formed in the phosphate glass matrix.

This research was supported by Grant No. INTAS 96-0677 (A.A.L.).

\*FAX: +7-812-247-1017.

Electronic address: andreev@aad.ioffe.rssi.ru

†FAX: +7-812-552-7954.

Electronic address: lipovskii@phtf.stu.neva.ru

<sup>1</sup>D.J. Norris, A.L. Efros, M. Rosen, and M.G. Bawendi, Phys. Rev. B **53**, 16 347 (1996).

<sup>2</sup>N.F. Borrelli and D.W. Smith, J. Non-Cryst. Solids **80**, 25 (1994).

<sup>3</sup>I. Kang and F.W. Wise, J. Opt. Soc. Am. B **14**, 1632 (1997).

<sup>4</sup>A.A. Lipovskii, E.V. Kolobkova, and V.D. Petrikov, Electron. Lett. **33**, 101 (1997).

<sup>5</sup>A. Lipovskii, E. Kolobkova, V. Petrikov, I. Kang, A. Olkhovets, T. Krauss, M. Thomas, J. Silcox, F. Wise, Q. Shen, and S. Kycia, Appl. Phys. Lett. **71**, 3406 (1997).

<sup>6</sup>C.B. Murray, D.J. Norris, and M.G. Bawendi, J. Am. Chem. Soc.

**115**, 8706 (1993).

<sup>7</sup>A.L. Efros and M. Rosen, Phys. Rev. B **58**, 7120 (1998).

<sup>8</sup>A.L. Efros and A.V. Rodina, Phys. Rev. B **47**, 10 005 (1993).

<sup>9</sup>A.L. Efros, Phys. Rev. B **46**, 7448 (1992).

<sup>10</sup>D.L. Mitchel and R.F. Wallis, Phys. Rev. **151**, 581 (1966).

<sup>11</sup>J.O. Dimmock, in *The Physics of Semimetals and Narrow-Gap Semiconductors*, edited by D.L. Carter and R.T. Bates (Pergamon Press, Oxford, 1971).

<sup>12</sup>L.D. Landau and E.M. Lifshiz, *Quantum Mechanics (Non-Relativistic Theory)*, 3rd ed. (Pergamon Press, Oxford, 1977).

<sup>13</sup>L.D. Landau and E.M. Lifshiz, *Lehrbuch der theoretischen Physik. Relativistische quantentheorie* (Akademie, Berlin, 1970).

<sup>14</sup>A.B. Migdal, *Qualitative Methods in Quantum Theory* (Benjamin, Reading, MA, 1977).